

Variable Switching Frequency Based Resonant Converter

¹Anooja Shahul, ²Prof. Annie P Oommen, ³Prof. Sera Mathew

¹PG Scholar, Dept. of EEE, Mar Athanasius College of Engineering, Kothamangalam, Kerala, India

²Professor, Dept. of EEE, Mar Athanasius College of Engineering, Kothamangalam, Kerala, India

³Assistant Professor, Dept. of EEE, Mar Athanasius College of Engineering, Kothamangalam, Kerala, India

Abstract: Energy from the sun and the wind can alleviate the pressure on traditional sources that has been considerably depleted. Many stages of renewable energy conversion require DC-DC converters with high voltage gain and high power. The applications where electrical isolation is not necessary, transformer less high gain converters can be used in order to avoid the difficulty of using large capacity transformers. This is a step up resonant converter which can achieve high voltage-gain using LC parallel resonant tank. Zero-voltage-switching (ZVS) of semiconductor devices in a resonant converter can be achieved by resonant devices. It is characterized by ZVS turn-on and nearly ZVS turn-off of main switches. Moreover, the equivalent voltage stress of the semiconductor devices is lower than other resonant step up converters. A resonant converter is simulated using MATLAB/SIMULINK and experimental results are also verified.

Keywords: Frequency Modulation, Resonant Converter, Zero Voltage Switching, Voltage Stress.

I. INTRODUCTION

At present, the voltages over the DC stages in the generation equipments of the renewable energy sources are relatively low, in the range of several hundred volts to several thousand volts, hence, high-power high-voltage step-up DC-DC converters are required to deliver the produced electrical energy to HVDC grid. Today's consumer equipment such as computers, fluorescent lights or LED lighting, households, businesses, industrial appliances and equipment need the DC power for their operation. Some renewable energy units generate in a DC way, so it is necessary to use DC-DC converters in mid stages. Step-up or boost converters are theoretically able to achieve infinitely high voltage conversion ratios; however, the maximum gain is practically limited by circuit imperfections, such as parasitic elements and switch commutation times. Resonant converters have been demonstrated to be a feasible option for high-voltage power converter. The disadvantage of the resonant converter is that it requires large capacity transformers [1]. This resonant converter has characteristics like ZVS turn ON and turns off, and also less voltage stress across semiconductor devices. With Zero-Voltage Switching (ZVS), converters exhibit lower switching loss and are widely used in many applications.

II. RESONANT CONVERTER

A resonant step-up DC-DC converter is studied, which can realize soft switching for main switches and diodes and large voltage-gain, and also has relatively lower equivalent voltage stress of the semiconductor devices and bidirectional magnetized resonant inductor. The operation principle of the converter is also discussed.

The resonant converter is shown in Fig. 1. The converter is composed of a full-bridge switch network, which is made up by Q_1 through Q_4 , a LC parallel resonant tank, a voltage doubler rectifier and two input blocking diodes, D_{b1} and D_{b2} . The operating waveforms are shown in Fig. 2 and detailed operation modes of the proposed converter are also explained. For the converter, Q_2 and Q_3 are tuned on and off simultaneously, Q_1 and Q_4 are tuned on and off simultaneously. For these switches, 180 degree phase shifted operation is carried out to realize ZVS. This LC resonant converter has ability to vary the gain depending on the switching frequency of the semiconductor switches.

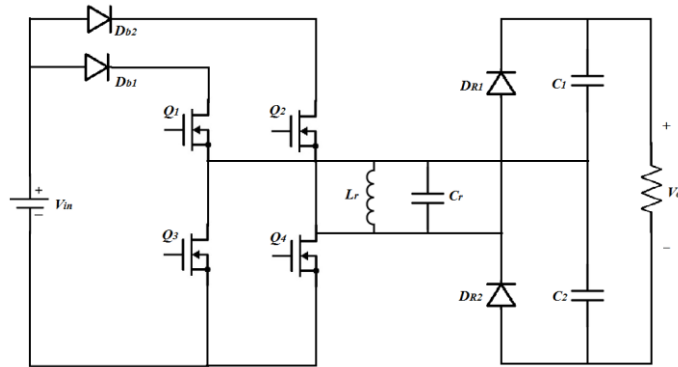


Fig.1: Circuit diagram

A. Modes of Operation:

(a). Mode 1 [t₀ - t₁]

During this mode, Q₁ and Q₄ are turned on resulting in the positive input voltage V_{in} across the LC parallel resonant tank, i.e.

$$v_{Lr} = v_{Cr} = V_{in}$$

Equivalent circuit of mode1 operation is shown in fig .3. The converter operates similar to a conventional Boost converter and the resonant inductor L_r acts as the Boost inductor with the current through it increasing linearly from I₀. The load is supplied by C₁ and C₂. At t₁, the resonant inductor current i_{Lr} reaches I₁.

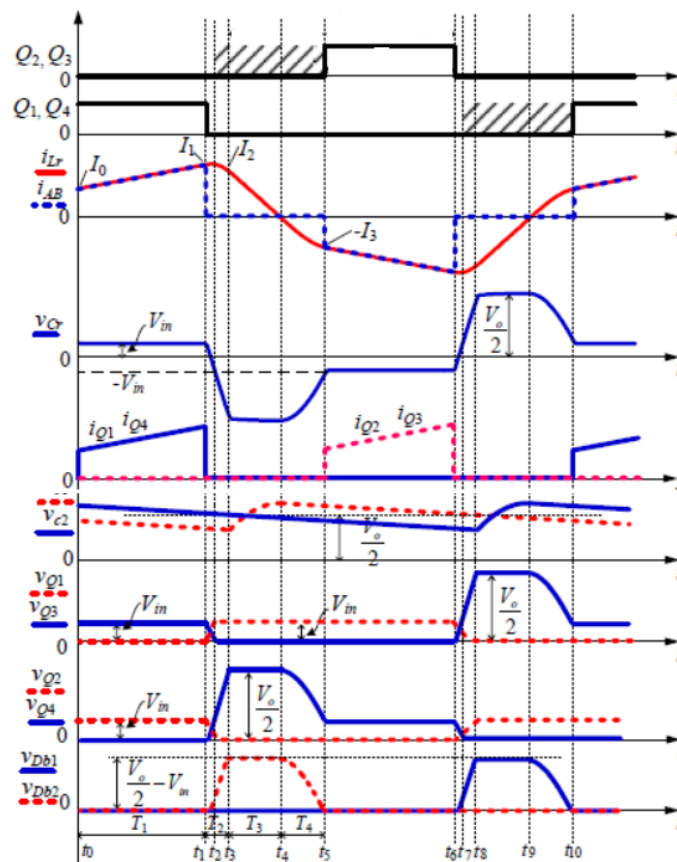


Fig. 2: Theoretical waveforms

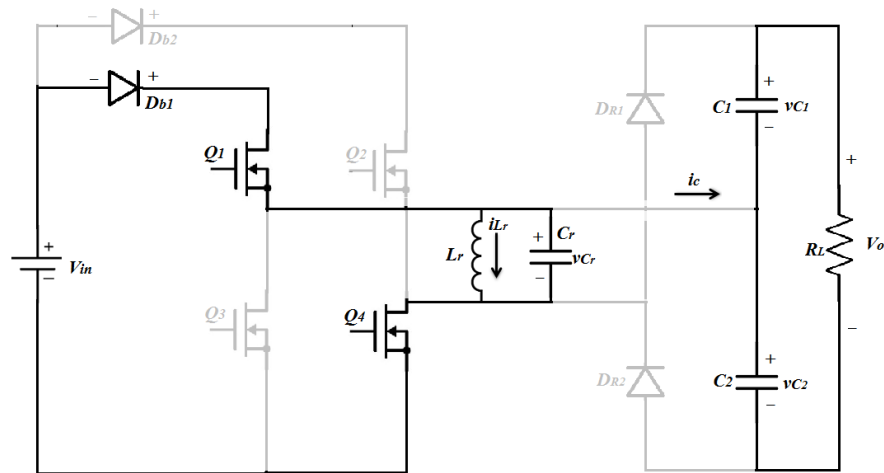


Fig. 3: Model operation

(b). Mode 2 [$t_1 - t_3$]

Mode 2 is divided into two regions : t_1-t_2 & t_2-t_3 . At t_1 , Q_1 and Q_4 are turned off and after that L_r resonates with C_r , v_{Cr} decreases from V_{in} and i_{Lr} increases from I_1 in resonant form. Taking into account the parasitic output capacitors of Q_1 through Q_4 and junction capacitor of D_{b2} , the equivalent circuit of the converter after t_1 is shown in Fig. 2, in which C_{Db2} , C_{Q1} and C_{Q4} are charged, C_{Q2} and C_{Q3} are discharged. In order to realize zero-voltage-switching (ZVS) for Q_2 and Q_3 , an additional capacitor, whose magnitude is about 10 times with respect to C_{Q2} , is connected in parallel with D_{b2} . Hence, the voltage across D_{b2} is considered unchanged during the charging/discharging process and D_{b2} is equivalent to be shorted. Due to C_r is much larger than the parasitic capacitances, the voltages across Q_1 and Q_4 increase slowly. As a result, Q_1 and Q_4 are turned off at almost zero voltage in this mode. When v_{Cr} drops to zero, i_{Lr} reaches its maximum magnitude. After that, v_{Cr} increases in negative direction and i_{Lr} declines in resonant form. At t_2 , $v_{Cr} = -V_{in}$, the voltages across Q_1 and Q_4 reach V_{in} , the voltages across Q_2 and Q_3 fall to zero and the two switches can be turned on under zero-voltage condition. The voltage across Q_1 is kept at V_{in} . The equivalent circuit of the converter after t_2 is shown in Fig. 5, in which D_2 and D_3 are the anti-parallel diodes of Q_2 and Q_3 , respectively. This mode runs until v_{Cr} increases to $V_o/2$, Q_4 reaches $V_o/2$ and the voltage across D_{b2} reaches $V_o/2 - V_{in}$.

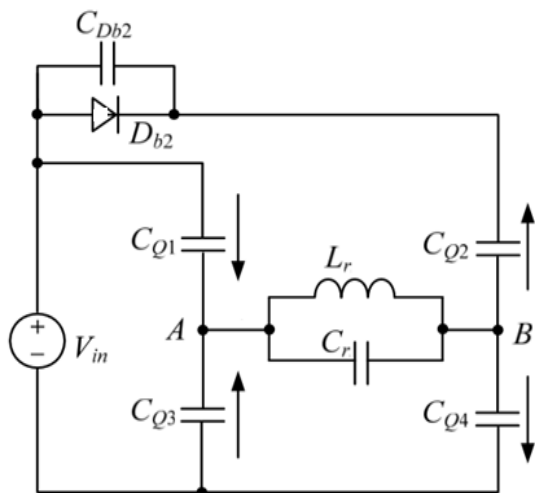


Fig. 4: Equivalent circuit of mode 2 [$t_1 - t_2$]

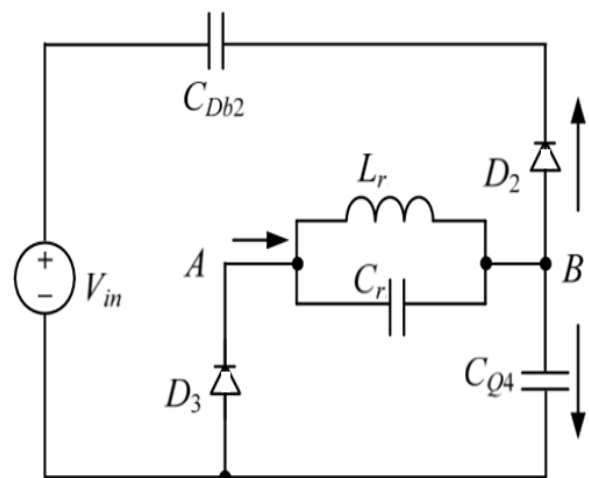


Fig. 5: Equivalent circuit of mode 2 [$t_2 - t_3$]

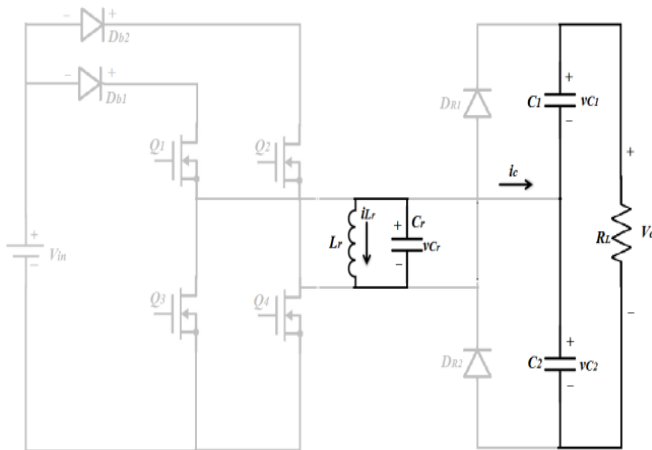


Fig. 6: Mode 2 operation

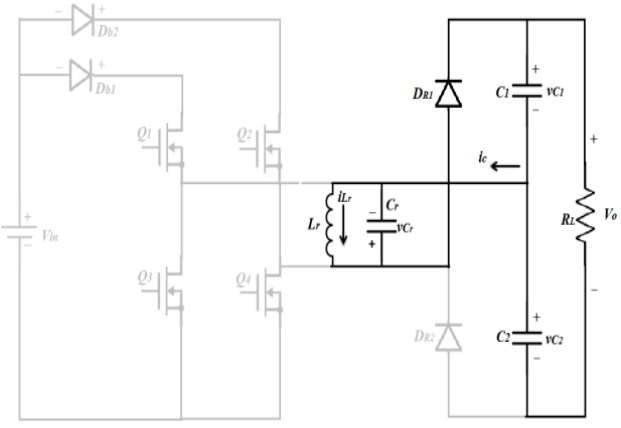


Fig. 7: Mode 3 operation

(c). Mode 3 [$t_3 - t_4$]

At t_3 , $v_{Cr} = -V_o/2$, D_{R1} conducts naturally, C_1 is charged by i_{Lr} through D_{R1} , v_{Cr} keeps unchanged, i_{Lr} decreases linearly. At t_4 , $i_{Lr} = 0$. Equivalent circuit of mode 3 operation is shown in fig. 7.

(d). Mode 4 [$t_4 - t_5$]

At t_4 , i_{Lr} decreases to zero and the current flowing through D_{R1} also decreases to zero, and D_{R1} is turned off, therefore, there is no reverse recovery. After t_4 , L_r resonates with C_r , C_r is discharged through L_r , v_{Cr} increases from $-V_o/2$ in positive direction, i_{Lr} increases from zero in negative direction. Equivalent circuit is shown in fig. 8. Meanwhile, the voltage across Q_4 declines from $V_o/2$. At t_5 , $v_{Cr} = -V_{in}$, $i_{Lr} = -I_3$.

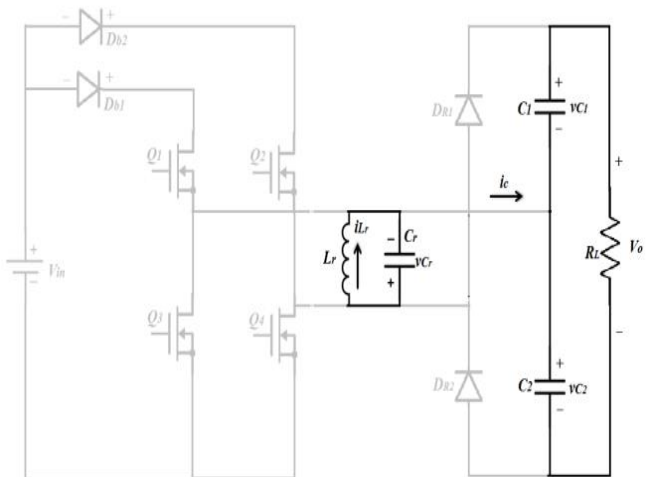


Fig. 8: Mode 4 operation

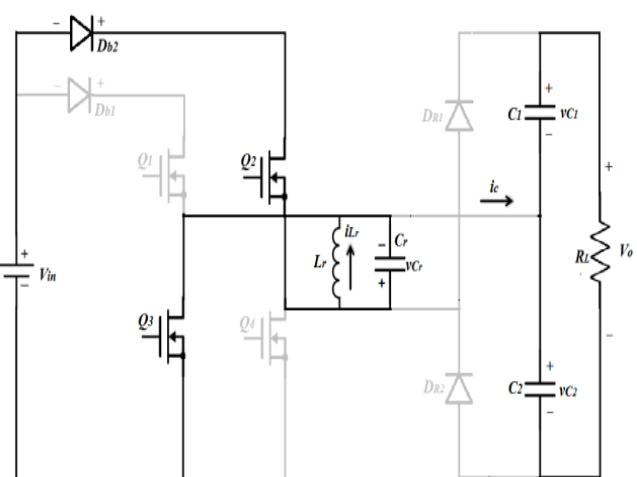


Fig. 9: Mode 5 operation

(e). Mode 5 [$t_5 - t_6$]

If Q_2 and Q_3 are turned on before t_5 , then after t_5 , L_r is charged by V_{in} through Q_2 and Q_3 , i_{Lr} increases in negative direction, the mode is similar to Mode 1. Equivalent circuit is shown in fig. 9.

The operation modes during [t_6, t_{10}] are similar to the modes 2, 3 and 4 and the only difference is in direction. During [t_6, t_{10}], Q_2 and Q_3 are turned off at almost zero voltage, Q_1 and Q_4 are turned on with ZVS.

III. SIMULATION MODEL AND RESULTS

In order to verify the operation principle and the theoretical analysis, a converter is simulated with MATLAB/SIMULINK simulation software and the simulation parameters are listed in Table.1. All switches using in simulation are ideal switches. Switching frequency is determined by the resonant parameters and here f_r is taken as 12kHz. Duty ratio is found as 0.35 from the analysis of the converter. The converter can operate below and above of the resonant frequency.

Table I: Simulation parameters

Input voltage V_{in}	20 V
Output voltage V_o	400 V
Resonant inductance L_r	124 μ H
Resonant capacitance C_r	1.5 μ F
Filter capacitance C_1, C_2	22 μ F
Duty cycle D	0.35

A. Control Strategy:

Control pulses for switch are generated by PWM method. Usually it is done by comparing a saw tooth carrier and a reference value. A repeating sequence of required frequency is compared with a constant 0.35, the duty ratio to generate a pulse with 35% ON time. Whenever repeating sequence is less than the constant, it will output a high value and if constant is smaller, it will output a low value. By varying the value of constant, duty ratio of MOSFET can be controlled. Out of four, two switches have same switching instants and remaining two have the same instants. Two pulses with 180 degree phase shifting is generated by the method of logical operations as shown in fig.13. Pulse output from the logic circuit is shown in Fig. 14.

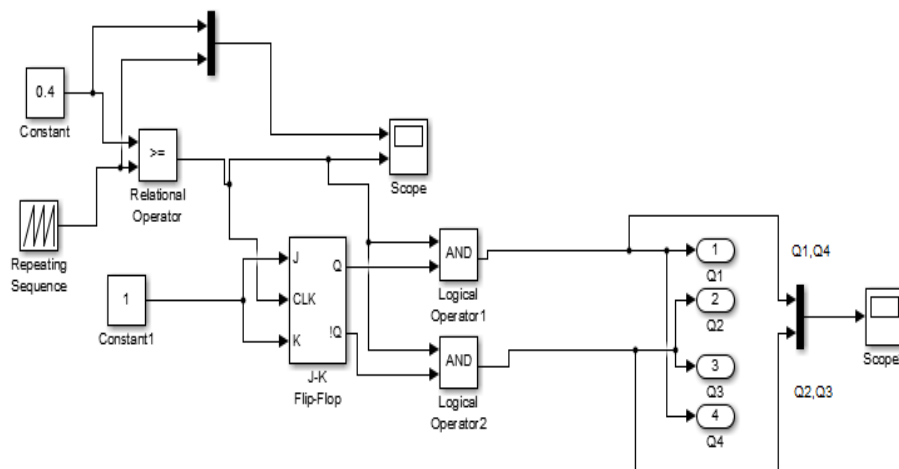


Fig. 13: Pulse generation circuit

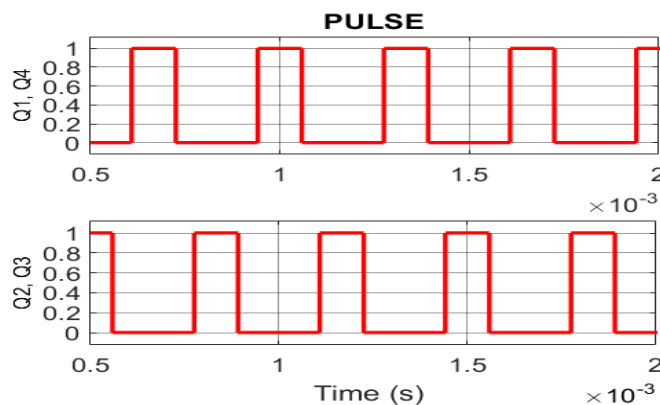


Fig. 14: Pulse output from logical circuit

B. Simulink Model:

Simulink model of step up resonant converter is shown in fig.15. MOSFET's are used as switches. Output voltage and stresses across switches are analyzed from the simulation results.

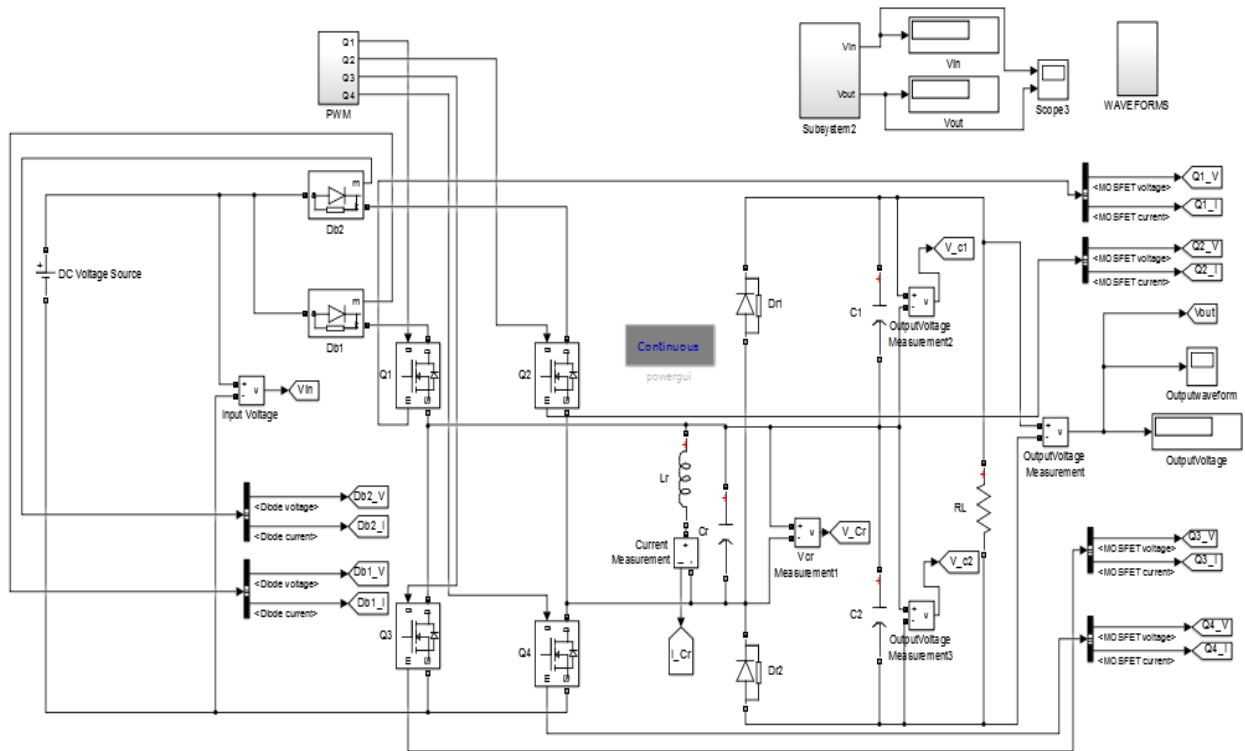


Fig. 15: Simulink model

C. Simulation Results:

Fig. 16(a, b) shows the simulation results at the input voltage 20V. At 3kHz, output voltage is 350V and at 11kHz , output voltage is 60V. Output voltage of step up converter is increasing as switching frequency is decreasing.

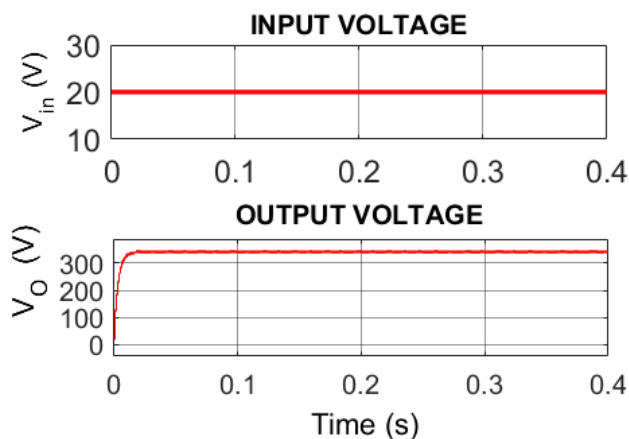


Fig. 16 (a): Output voltage (Vo) at fs = 3kHz

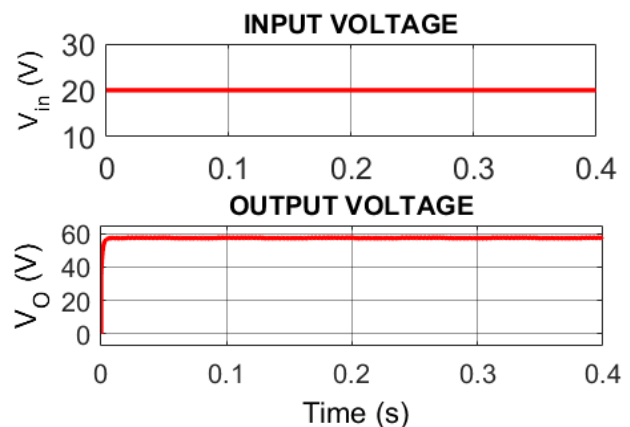


Fig. 16 (b): Output voltage (Vo) at fs = 11kHz

As shown in fig. 18 and fig. 19, the voltage stress of Q1 and Q2 is Vo/2, the voltage stresses of Q3 and Q4 is also less compared to output voltage. The peak voltage across the LC resonant tank is Vo/2, only half of the output voltage and hence voltage rating of capacitor can be taken as half of output voltage.

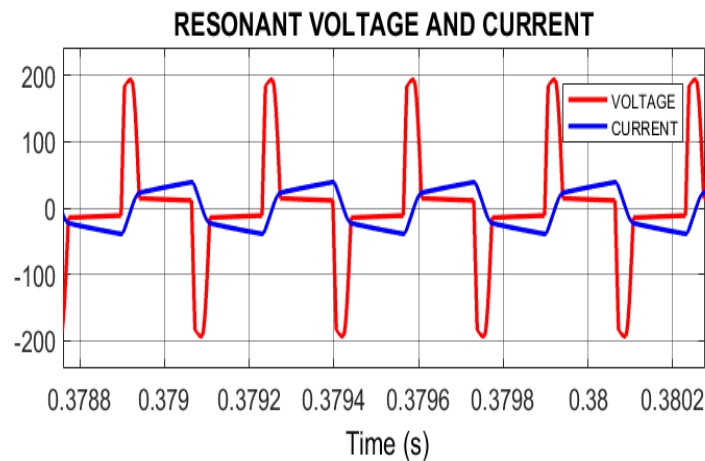


Fig. 17: Resonant voltage & current

From the fig. 18 and fig. 19, it can be seen that, Q_1 through Q_3 are turned on under zero voltage condition and when they are turned off, the voltage across the device increases slowly from zero. Thus from the simulation results, it is verified that switches are turned on at zero voltage and turned off nearly at zero voltage.

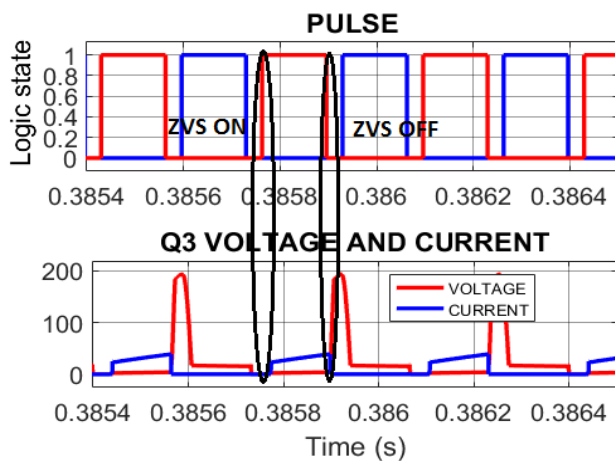


Fig. 18: ZVS of Q_3 (lower switch)

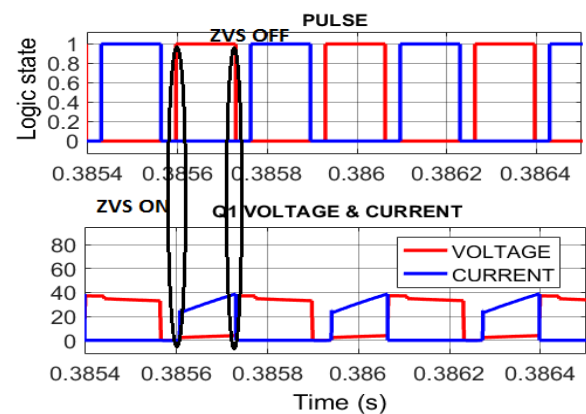


Fig. 19: ZVS of Q_1 (upper switch)

Fig. 20 and fig. 21 shows the efficiency curves of resonant converter. Fig. 20 shows the efficiency at different output loads and fig. 21 shows the efficiency at different input voltages. It can be seen (Fig. 21) that efficiency can be up to 95.5%.

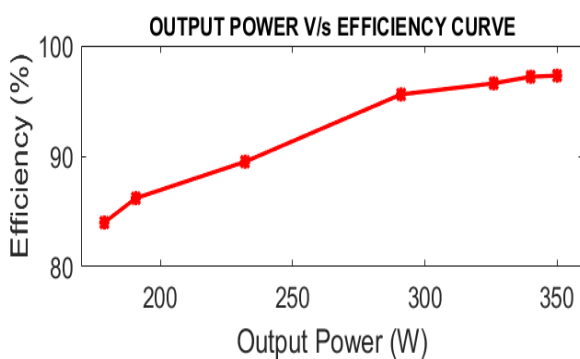


Fig. 20: Efficiency at different output power

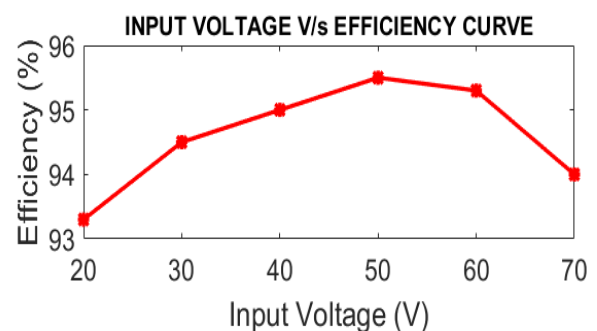


Fig. 21: Efficiency at different input voltage

IV. CONCLUSIONS

The resonant DC-DC converter which can achieve very high step-up voltage gain (about 10 to 20 times) and it is suitable for high-power high-voltage applications. The converter utilizes the resonant inductor to deliver power by charging from the input and discharging to the output. The resonant capacitor is employed to achieve zero-voltage turn-on and turn-off for the active switches and ZCS for the rectifier diodes. The parameters of the resonant tank determine the maximum switching frequency, the range of switching frequency and current ratings of active switches and diodes. The converter is controlled by the variable switching frequency. Simulation results verify the operation principle of the converter and parameters selection of the resonant tank.

REFERENCES

- [1] Shixiong Fan, Weiwei Ma, Tee Chong Lim, Barry Wayne Williams, "Design and control of a wind energy conversion system based on a resonant dc/dc converter", *IET Renewable Power Generation*, vol. 7, iss. 3, pp. 265-274, 2013.
- [2] Kiwoo Park, "Analysis and Design of a Parallel Connected Single Active Bridge DC-DC Converter for High-Power Wind Farm Applications", *Aalborg University*, 2013.
- [3] Nicholas Denniston, Ahmed M. Massoud, Shehab Ahmed, Member and Prasad. Enjeti, "Multiple-Module High-Gain High-Voltage DC-DC Transformers for Offshore Wind Energy Systems", *IEEE Transactions on Power Electronics*, vol.58, no. 5, May 2011.
- [4] Xinbo Ruan, "A Novel Zero-Voltage and Zero-Current-Switching PWM Full-Bridge Converter Using Two Diodes in Series With the Lagging Leg", *IEEE Transactions on Industrial Electronics*, vol. 48, no. 4, August 2001.
- [5] Hamidreza Keyhani, and Hamid A. Toliyat, "Partial-Resonant BuckBoost and Flyback DCDC Converters", *IEEE Transactions on Power Electronics*, vol. 29, no. 8, August 2014.
- [6] Wu Chen, Member, Xiaogang Wu, Liangzhong Yao, Wei Jiang, and Renjie Hu, "A Step-up Resonant Converter for Grid-Connected Renewable Energy Sources", *IEEE Transactions on Power Electronics*, 2013.
- [7] Hamidreza Keyhani and Hamid A. Toliyat, "Isolated ZVS High-Frequency-Link AC-AC Converter With a Reduced Switch Count", *IEEE Transactions on Power Electronics*, vol. 29, no. 8, August 2014.
- [8] Zhiliang Zhang¹, Fei-Fei Li¹, and Yan-Fei Liu², "A High Frequency Dual-Channel Isolated Resonant Gate Driver with Low Gate Drive Loss for ZVS Full-Bridge Converters", *IEEE*, 2014.
- [9] Suk-Ho Ahn, Hong-Je Ryoo, Ji-Woong Gong, and Sung-Roc Jang, "Design and Test of a 35 kJ/s High-Voltage Capacitor Charger Based on a Delta-Connected Three-Phase Resonant Converter" *IEEE Transactions on Power Electronics*, vol. 29, no. 8, August 2014.
- [10] Fujin Deng and Zhe Chen, "Control of Improved Full-Bridge Three-Level DC/DC Converter for Wind Turbines in a DC Grid" *IEEE Transactions on Power Electronics*, vol. 28, no. 1, January 2013.